JACS
JOURNAL OF THE AMERICAN CHEMICAL SOCIETY
Communication
pubs.acs.org/JACS

Enhancing the Efficiency of Gold Nanoparticles Treatment of Cancer by Increasing Their Rate of Endocytosis and Cell Accumulation Using Rifampicin

Moustafa R. K. Ali,[‡] Sajanlal R. Panikkanvalappil,[‡] and Mostafa A. El-Sayed*

Laser Dynamics Laboratory, School of Chemistry and Biochemistry, Georgia Institute of Technology, Atlanta, Georgia 30332-0400, United States

Supporting Information

ABSTRACT: To minimize the toxicity of gold nanoparticles (AuNPs) in cancer treatment, we have developed a technique, which utilizes lesser amount of AuNPs while exhibiting increased treatment efficiency. Rifampicin (RF) is known for its ability to enhance the accumulation of anticancer drugs in multidrug resistant (MDR) cancer cells. In this work we have shown that RF-conjugated AuNPs can greatly enhance the rate as well as efficiency of endocytosis of NPs and hence their concentration inside the cancer cell. Cell viability results showed a remarkable enhancement in the photothermal therapeutic effect of Au nanorods in presence of RF. This is expected to decrease the demand on the overall amount of AuNPs needed for treating cancer and thus decreasing its toxicity.

Cancer, often described as one of the most dreadful diseases, still remains as an important challenge across the world. Enhancing the efficiency of delivering anticancer drugs precisely to the cancer sites is critical for its successful treatment.[1,2] Hence, ongoing cancer researches are keenly focused on identifying innovative ways to enhance the targeting efficiency of targeting nanoparticles so as to elevate the rate of endocytosis and hence to decrease toxicity. Though nanotechnology-based methods have showed promising results in view of screening cancer cells[3−5] and targeted drug delivery,[6−8] it is still challenging to bypass the efflux of drug carrying nanoparticles through multidrug resistance (MDR) mechanism[9−11] in cancer cells. In view of minimizing the toxicity during the AuNPs-based plasmonic chemotherapy, it is highly desirable to develop novel functionalized nanomaterials, which could effectively deliver the drug carrying NPs into the cancer cells, without being accumulated outside the cells.

Among NPs, gold nanorods (AuNRs) are considered as efficient drug delivery platform owing to their unique optical and photothermal properties.[6,12] Though molecules such as PEG, PNIPAM, SiO_2, etc. are known[1,6,13,14] for passivation of AuNRs against its toxic effect and for carrying the drug to the target cells, proteins are considered to be more convenient and efficient carrier systems as they can accommodate more drug molecules per protein molecules and due to their biocompatible nature.[15,16] The concept of plasmonic chemotherapy[17−20] using AuNRs carrying anticancer drug molecules as an efficient drug delivery vehicle has greater relevance in this regard. Rifampicin (RF), an antibiotic used to treat infections, is known for its ability to bypass the MDR in cancer cells.[21,22] Here, we have shown that RF-loaded AuNRs can enhance the rate and efficacy of endocytosis of paclitaxel (Ptxl) (an anticancer drug molecule)-carrying AuNRs into the cancer cells. Moreover, the fast endocytosis of the NPs could be an attractive treatment modality, which could decrease the possibility of targeted NPs being excreted through extracellular fluids during their intravenous administration.

As a drug carrier system, bovine serum albumin (BSA) has been used to conjugate AuNRs due to their excellent biocompatibility, low cost and presence of two binding sites.[16,23,24] For this study, we used two different AuNR systems: small AuNRs (sAuNRs)[25] (17 nm length and 3.5 nm diameter) and bigger AuNRs (bAuNRs) (47 nm length and 10 nm diameter). Conjugations of BSA with these NRs were obvious from their extinction spectra, as the NRs solutions showed a distinct red shift in their absorption maxima after binding with BSA (Figure 1A,B). TEM images of AuNRs used in this study are also given in Figure 1D,E. Binding of RF molecules with BSA-conjugated AuNRs (AuNRs@BSA) was confirmed fluorometrically, which showed a distinct reduction in the fluorescence emission (~350 nm) intensity (excitation at 280 nm) as well as slight shift in their emission maximum after the addition of 10^{-4} M of RF solution into AuNRs@BSA (see Supporting Information (SI) 2). RF and Ptxl binding was also obvious in pure BSA solution (SI 3 and 4) though the excitation maximum was red-shifted to 294 nm (SI 4). The observed red shift in fluorescence emission of BSA after RF binding can be attributed to an increased polarity of the region surrounding the tryptophan site,[26] whereas quenching of fluorescence is mainly due to the energy transfer by the intermolecular interaction of drug molecules with tryptophan moiety present in the close proximity of drug binding site in BSA.[27,28]

To study the efficiency of drug release for each nanorods (sAuNRs and bAuNRs), we used RF-loaded AuNRs@BSA (AuNRs@BSA-RF). The charge transfer band of RF[29] found at 474 nm red-shifted to 482 nm after addition into sAuNRs@BSA (Figure 1C), which clearly suggests the binding of RF with sAuNRs@BSA. Drug release was triggered by irradiating the AuNRs@BSA-RF solutions with a CW laser source with excitation wavelength of 808 nm, which overlaps with the

Received: December 13, 2013
Published: January 27, 2014

dx.doi.org/10.1021/ja4124412 | J. Am. Chem. Soc. 2014, 136, 4464−4467

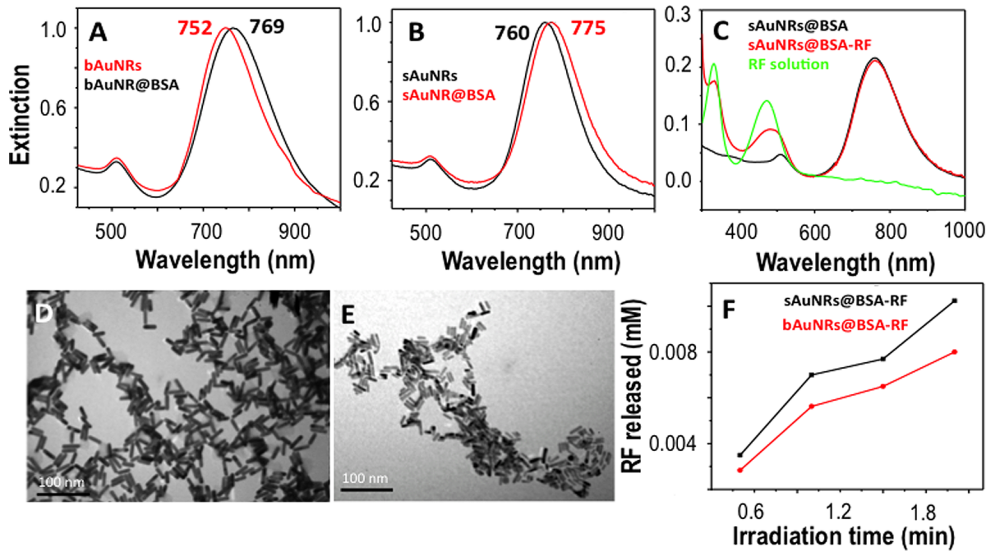

Figure 1. (A, D) and (B, E) are the extinction spectra and TEM images of bAuNRs and sAuNRs, respectively. Extinction spectra of AuNRs@BSA are also given. (C) Extinction spectra of sAuNRs@BSA and sAuNRs@BSA-RF. Absorption spectrum of pure RF solution (green trace) is also given. (F) Plots showing the concentrations of RF released from bAuNRs@BSA-RF and sAuNRs@BSA-RF upon laser exposure.

longitudinal surface plasmon resonance (LSPR) bands of both sAuNRs@BSA-RF and bAuNRs@BSA-RF (Figure 1A,B). The concentrations of liberated RF after laser irradiation was calculated using the extinction coefficient of RF and the absorption at 334 nm. We found that, each bAuNRs@BSA contains ~95 RF molecules on its surface. The high payload capacity has been attributed to the presence of protein corona around the NR.[16,30] Photothermal studies suggest an enhancement in drug release for sAuNRs@BSA-RF compared to bAuNRs@BSA-RF, when the nanorod solutions of similar optical densities (ODs) were used. A plot of laser irradiation time versus amount of RF released from both sAuNRs@BSA-RF and bAuNRs@BSA-RF at different irradiation time is shown in Figure 1F. Due to their higher absorption and lower scattering properties, sAuNRs are considered to be a good candidate in plasmonic chemotherapy. Enhanced drug release capability of sAuNRs@BSA-RF is attributed to their higher efficiency in generating heat upon laser irradiation compared to the bAuNRs@BSA-RF of similar optical density. While laser irradiation of bAuNRs@BSA-RF (OD = 1) for 2 min resulted in the enhancement of the temperature from 27 to 65 ± 0.5 °C, that of sAuNRs@BSA-RF (OD = 1) resulted in an increase of the solution temperature from 27 to 82 ± 0.5 °C. A similar experiment using RF-loaded Au@citrate nanospheres (AuNSs@BSA-RF) yielded no significant enhancement in the temperature owing to mismatch between the laser excitation source (808 nm) and their surface plasmon resonance band (525 nm) (SI 5). Further, the conjugation of RF and Ptxl with AuNRs@BSA was confirmed by surface enhanced Raman spectroscopic (SERS) studies (SI 6 and 7).

For the cellular uptake study, we used RGD (arginine-glycine-aspartic acid peptide)-functionalized bAuNRs@BSA (bAuNRs@BSA@RGD) (more details on the synthesis is given in SI 1). RGD can effectively target $\alpha_v\beta_6$ integrins on the human squamous carcinoma (HSC) cell surface[31] and can enter to the cytoplasm via receptor-mediated endocytosis. Rate of their uptake was monitored using dark-field (DF) microscopy. A schematic is given in Figure 2A.

The DF images of the HSC cells incubated with 0.1 nM bAuNRs@BSA@RGD, at various time intervals such as 0.5, 2, and 24 h, respectively, are given in Figure 2B–D. From the images, it is clear that the uptake is minimal even after 2 h of incubation and most of the NRs were confined to the cell membrane and partially to the cytoplasm (Figure 2C). As the number of NRs internalized was very less, the intensity of scattering from the NRs was poor and the cells appeared dark. At the same time, the cells incubated with 19:1 mixture of 0.1 nM of bAuNRs@BSA@RGD and 0.1 nM of bAuNRs@BSA-

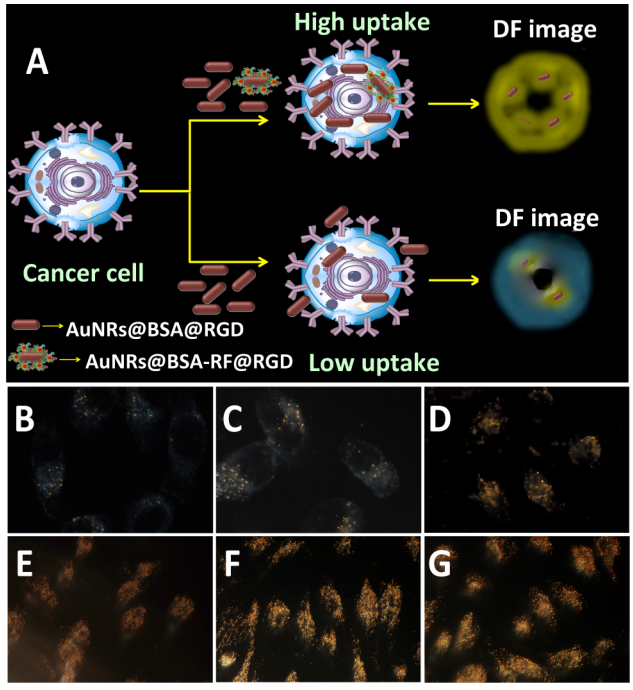

Figure 2. (A) Schematic showing the influence of bAuNRs@BSA-RF@RGD on the AuNRs uptake. (B–D) DF images of HSC cells collected at 0.5, 2, and 24 h, respectively, during the uptake of bAuNRs@BSA@RGD (0.1 nM). (E–G) DF images of HSC cells collected at 0.5, 2, and 24 h, respectively, during uptake of 19:1 solution of bAuNRs@BSA@RGD (0.1 nM) and bAuNRs@BSA-RF@RGD (0.1 nM).

dx.doi.org/10.1021/ja4124412 | J. Am. Chem. Soc. 2014, 136, 4464–4467

RF@RGD solutions showed remarkably high uptake even after 30 min and the NRs were distributed throughout the intracellular components (Figure 2E). These cells appeared bright due to the intense scattering from large number of endocytosed NRs. Moreover, in presence of bAuNRs@BSA-RF@RGD, endocytosis of bAuNRs@BSA@RGD was almost complete within 2 h of incubation and no drastic change in the intensity of scattering of NRs was observed after 24 h. This indicates that presence of even 5% of RF-containing bAuNRs@BSA-RF@RGD in the total volume of AuNRs solution can make a huge enhancement in the rate as well as the efficiency of endocytosis of the NPs. The experiments were conducted by keeping the total amount of AuNRs constant. We did not use sAuNRs for uptake study, as the scattering was negligible for sAuNRs due to their smaller size. The role of bAuNRs@BSA-RF@RGD in enhancing the efficiency of photothermal therapeutic effect was further confirmed by conducting various cell viability experiments (see later). The capability of bAuNRs@BSA-RF@RGD in enhancing the endocytosis of NPs can be attributed to the chemo-sensitizing activity[22,32,33] of RF by down regulating the activity of MDR plasma membrane protein (P-glycoprotein).

The cell viability data showed a drastic decrease in the percentage of viability (~30%) for the HSC cells incubated with bAuNRs@BSA-RF@RGD (0.1 nM) after exposing to the laser (808 nm) for 2 min (Figure 3A). At the same time, the viability was around 80% for the cells treated with bAuNRs@BSA@RGD after 2 min laser exposure (Figure 3A). The higher killing efficiency in the former case is attributed to the faster endocytosis and high accumulation of AuNRs in the cancer cells by the influence of RF and subsequent enhancement in the resultant heat generated inside the cell and the medium during the laser exposure. Among the nanorods, sAuNRs@BSA-RF@RGD exhibited higher efficiency in killing the cancer cells (viability~20%), when exposed to laser (Figure 3B). At similar conditions, with sAuNRs@BSA@RGD the cell viability was nearly 70%.

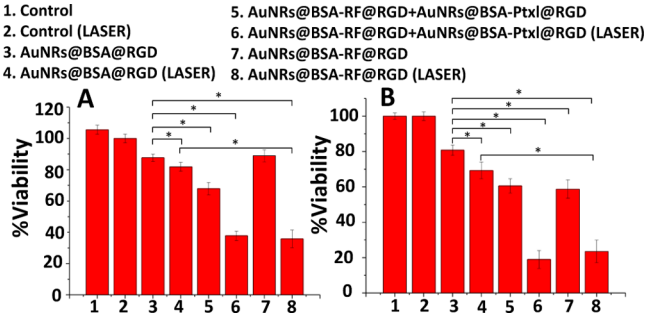

Figure 3. Cell viability results for the exposure of HSC cells to 0.1 nM of AuNRs solutions of different sizes and functionalities (A) for bAuNRs and (B) for sAuNRs. Statistical significance has been indicated by * (p-value <0.05).

To study the influence of RF in the plasmonic chemotherapy, we administrated Ptxl-loaded AuNRs (bAuNRs@BSA-Ptxl@RGD) along with 5% bAuNRs@BSA-RF@RGD to the HSC cells and these were exposed to the laser for 2 min. The cell viability value was around 30% in this case. When the experiment was conducted under similar conditions with sAuNRs instead of bAuNRs, the viability was around 18% (Figure 3B), which has been attributed to the enhanced accumulation of sAuNRs by the influence of RF and subsequent photothermal effect as well as the chemotherapeutic nature of sAuNRs@BSA-Ptxl@RGD. Note that the viability was around 70% for the cells with sAuNRs@BSA@RGD under laser exposure.

In conclusion, we showed that RF could enhance the rate and internalization of AuNRs more effectively into the cancer cells. Fast and enhanced endocytosis of NPs inside the cells during this approach was probed using DF microscopy. Cell viability studies have demonstrated the advantages of this approach over conventional plasmonic chemotherapy. The current method has great impact in conquering new avenues in bypassing MDR in various cancer cells and thereby to decrease the demand on the overall concentration of gold NPs needed for plasmonic chemotherapy.

■ ASSOCIATED CONTENT

Supporting Information

Detailed experimental procedure, fluorescence spectra showing the drug binding with BSA, additional supporting SERS spectra, extinction spectra and TEM images. This material is available free of charge via the Internet at http://pubs.acs.org.

■ AUTHOR INFORMATION

Corresponding Author

melsayed@gatech.edu

Author Contributions

‡These authors contributed equally.

Notes

The authors declare no competing financial interest.

■ ACKNOWLEDGMENTS

This work was supported by NSF-DMR grant (1206637).

■ REFERENCES

(1) Wang, A. Z.; Langer, R.; Farokhzad, O. C. *Annu. Rev. Med.* **2012**, *63*, 185.
(2) Chow, E. K.; Zhang, X.-Q.; Chen, M.; Lam, R.; Robinson, E.; Huang, H.; Schaffer, D.; Osawa, E.; Goga, A.; Ho, D. *Sci. Transl. Med.* **2011**, *3*, 73ra21.
(3) Dreaden, E. C.; El-Sayed, M. A. *Acc. Chem. Res.* **2012**, *45*, 1854.
(4) Panikkanvalappil, S. R.; Mackey, M. A.; El-Sayed, M. A. *J. Am. Chem. Soc.* **2013**, *135*, 4815.
(5) Panikkanvalappil, S. R.; Mahmoud, M. A.; Mackey, M. A.; El-Sayed, M. A. *ACS Nano* **2013**, *7*, 7524.
(6) Dreaden, E. C.; Mackey, M. A.; Huang, X.; Kang, B.; El-Sayed, M. A. *Chem. Soc. Rev.* **2011**, *40*, 3391.
(7) Davis, M. E.; Chen, Z.; Shin, D. M. *Nat. Rev. Drug Discovery* **2008**, *7*, 771.
(8) Dykman, L.; Khlebtsov, N. *Chem. Soc. Rev.* **2012**, *41*, 2256.
(9) Szakacs, G.; Paterson, J. K.; Ludwig, J. A.; Booth-Genthe, C.; Gottesman, M. M. *Nat. Rev. Drug Discovery* **2006**, *5*, 219.
(10) Persidis, A. *Nat. Biotechnol.* **1999**, *17*, 94.
(11) Wang, F.; Wang, Y.-C.; Dou, S.; Xiong, M.-H.; Sun, T.-M.; Wang, J. *ACS Nano* **2011**, *5*, 3679.
(12) Dreaden, E. C.; Austin, L. A.; Mackey, M. A.; El-Sayed, M. A. *Ther. Delivery* **2012**, *3*, 457.
(13) Mackowiak, S. A.; Schmidt, A.; Weiss, V.; Argyo, C.; von Schirnding, C.; Bein, T.; Bräuchle, C. *Nano Lett.* **2013**, *13*, 2576.
(14) Shen, Y.; Jin, E.; Zhang, B.; Murphy, C. J.; Sui, M.; Zhao, J.; Wang, J.; Tang, J.; Fan, M.; Van Kirk, E.; Murdoch, W. J. *J. Am. Chem. Soc.* **2010**, *132*, 4259.
(15) MaHam, A.; Tang, Z.; Wu, H.; Wang, J.; Lin, Y. *Small* **2009**, *5*, 1706.
(16) Au, K. M.; Armes, S. P. *ACS Nano* **2012**, *6*, 8261.

(17) Lukianova-Hleb, E. Y.; Ren, X.; Zasadzinski, J. A.; Wu, X.; Lapotko, D. O. *Adv. Mater.* **2012**, *24*, 3831.
(18) Ren, F.; Bhana, S.; Norman, D. D.; Johnson, J.; Xu, L.; Baker, D. L.; Parrill, A. L.; Huang, X. *Bioconjugate Chem.* **2013**, *24*, 376.
(19) Zheng, M.; Yue, C.; Ma, Y.; Gong, P.; Zhao, P.; Zheng, C.; Sheng, Z.; Zhang, P.; Wang, Z.; Cai, L. *ACS Nano* **2013**, *7*, 2056.
(20) Dickerson, E. B.; Dreaden, E. C.; Huang, X.; El-Sayed, I. H.; Chu, H.; Pushpanketh, S.; McDonald, J. F.; El-Sayed, M. A. *Cancer Lett.* **2008**, *269*, 57.
(21) Kim, H.-S.; Min, Y.-D.; Choi, C.-H. *Biochem. Biophys. Res. Commun.* **2001**, *283*, 64.
(22) Courtois, A.; Payen, L.; Vernhet, L.; de Vries, E. G. E.; Guillouzo, A.; Fardel, O. *Cancer Lett.* **1999**, *139*, 97.
(23) Khullar, P.; Singh, V.; Mahal, A.; Dave, P. N.; Thakur, S.; Kaur, G.; Singh, J.; Singh Kamboj, S.; Singh Bakshi, M. *J. Phys. Chem. C* **2012**, *116*, 8834.
(24) Dominguez-Medina, S.; Blankenburg, J.; Olson, J.; Landes, C. F.; Link, S. *ACS Sustainable Chem. Eng.* **2013**, *1*, 833.
(25) Ali, M. R. K.; Snyder, B.; El-Sayed, M. A. *Langmuir* **2012**, *28*, 9807.
(26) Yu, O.-Y.; Cheng, Y.-F.; Huang, S.-Y.; Bai, A.-M.; Hu, Y.-J. *J. Solution Chem.* **2011**, *40*, 1711.
(27) Kamat, B.; Seetharamappa, J. *J. Chem. Sci.* **2005**, *117*, 649.
(28) Agudelo, D.; Bourassa, P.; Bruneau, J.; Bérubé, G.; Asselin, É.; Tajmir-Riahi, H.-A. *PLoS One* **2012**, *7*, e43814.
(29) Howes, B. D.; Guerrini, L.; Sanchez-Cortes, S.; Marzocchi, M. P.; Garcia-Ramos, J. V.; Smulevich, G. *J. Raman Spectrosc.* **2007**, *38*, 859.
(30) Kah, J. C. Y.; Chen, J.; Zubieta, A.; Hamad-Schifferli, K. *ACS Nano* **2012**, *6*, 6730.
(31) Kang, B.; Mackey, M. A.; El-Sayed, M. A. *J. Am. Chem. Soc.* **2010**, *132*, 1517.
(32) Fardel, O.; Lecureur, V.; Loyer, P.; Guillouzo, A. *Biochem. Pharmacol.* **1995**, *49*, 1255.
(33) Shichiri, M.; Fukai, N.; Kono, Y.; Tanaka, Y. *Cancer Res.* **2009**, *69*, 4760.